Terahertz Laser Spectroscopy of the Water Pentamer: Structure and Hydrogen Bond Rearrangement Dynamics

K. Liu,† M. G. Brown, J. D. Cruzan, and R. J. Saykally*

Department of Chemistry, University of California, Berkeley, California 94720

Received: March 3, 1997; In Final Form: August 11, 1997[⊗]

The detailed analysis of a parallel vibration−rotation-tunneling (VRT) band of the isolated cyclic perdeuterated (d_{10}) water pentamer measured near 2.4 THz (81.2 cm^{-1}) is presented. The vibrationally averaged rotational constants correspond rigorously to those of a quasiplanar (C_{5h}) oblate top whereas the equilibrium cyclic structure is predicted to be slightly asymmetric due to puckering of the oxygen framework and uneven distribution of the free O−D bonds above and below the ring. The vibrational averaging which underlies the symmetric top behavior, the absence of a first-order Stark effect, as well as the origin of the observed intermolecular vibration, is consequently rationalized using a five-dimensional model of the pseudorotation, analogous to that established for the water trimer. Pseudorotation is induced by the nearly barrierless "flipping" of the monomers about their donor hydrogen bonds and by accompanying hydrogen bond network puckering motions. The observed vibration is tentatively assigned to the k (pseudorotational quantum number) = 5 (upper) ← 0 pseudorotational transition classified under the cyclic molecular symmetry group G_{10} (isomorphic to C_{5h}); new transitions are also predicted from this model. The donor (bifurcation) tunneling responsible for the spectral splittings observed in each pseudorotational state in the water trimer does not produce observable splittings in the pentamer-d_{10}, but is predicted to do so for the normal isotopic pentamer-h_{10}. The experimentally deduced inter-oxygen separations for water clusters up to the pentamer (for which the vibrationally averaged result is R_{O-O} = 2.76 Å) as a function of the cluster size exhibit exponential contraction toward the corresponding distance in ice Ih.

I. Introduction

A recent surge of progress in laser spectroscopy[1−11] and ab initio,[12−29] semiempirical,[30−34] and diffusion Monte Carlo simulation[35−37] studies of small water clusters has characterized the structures and hydrogen-bond rearrangement (HBR) dynamics[18,19,38−42] in these systems in great detail. The information extracted from this work, e.g., characterization of the cooperative interactions) is likely to have important consequences for enhancing our understanding of aqueous processes in chemistry and biology.[43,44] While the water dimer has previously been shown[45−47] to adopt a trans-linear hydrogen bonding configuration, experimental structures of the trimer,[3] tetramer,[8] and pentamer[9] correspond to *symmetric* quasiplanar oblate rotors. In the trimer and pentamer, this is a result of vibrational averaging caused by the facile "flipping" motions of the free protons over the degenerate *asymmetric* equilibrium conformations predicted by theory, whereas the tetramer has an S_4 equilibrium structure. Both experiment[10] and theory[22] agree that a structural transition occurs at a cluster size of 6, wherein these quasi two-dimensional (2-D) cyclic rings become less stable than 3-D noncyclic hydrogen bonding networks as a consequence of the competition between maximizing the number of hydrogen bonds and minimizing the strains within the cluster. The HBR dynamics occurring in these systems have been characterized as (1) low-frequency torsional motions corresponding to the slightly hindered rotations (flipping) of monomers about their donor O−H bonds and (2) high-barrier tunneling (donor tunneling: exchange of the free and H-bonded protons within a given monomer) that involves breaking and forming of the hydrogen bonds; the latter has a transition state corresponding to a bifurcated H-bond configuration and is also referred to as "bifurcation" tunneling.[18,42] Much of the present experimental evidence is provided by tunable terahertz laser vibration−rotation-tunneling (VRT) spectroscopy, as reviewed recently.[11]

The quasiplanar hydrogen-bonded water polygons in general, as well as pentagons in particular, may be of general significance in the aqueous solvation of bio-macromolecules,[48−50] in hydration of small hydrophobes into clathrates,[51] as well as in explaining the anomalous thermodynamic properties of the liquid.[52] The special role of cyclic pentamers in bulk water systems[53−55] relates to the nearly optimum tetrahedral O−O−O bond angles achieved in this configuration.[54]

Our initial characterization[9] of the water pentamer agrees with the early experimental[56] and theoretical investigations[15,25,30,31,57−60] in that the most stable structure is a cyclic, slightly puckered ring with each monomer acting as a single donor and single acceptor (Figure 1). In this paper, we present the details of the structure determination. Experimental vibrationally averaged structural properties, e.g., the interoxygen distance, have been extracted from the measured rotational constants for water clusters ranging from dimer to the noncyclic hexamer and are subsequently compared with theoretical predictions. However, the spectroscopic details revealed by our experiment require analysis transcending a description of only the equilibrium structure. As a second emphasis of the present work, we address the HBR dynamics evident in the pentamer rovibrational spectrum, as also found for the trimer[3−6] and tetramer.[8]

Wales and Walsh (W&W)[61] have first characterized the flipping and bifurcation tunneling pathways in the water pentamer using ab initio calculations and a number of empirical potentials. On the basis of the estimated tunneling splittings associated with the two rearrangement mechanisms, these authors reasoned that the lack of such splittings in the previous

† Present address: Department of Chemistry, University of Southern California.

* To whom correspondence should be addressed.

⊗ Abstract published in *Advance ACS Abstracts,* October 1, 1997.

S1089-5639(97)00781-0 CCC: $14.00

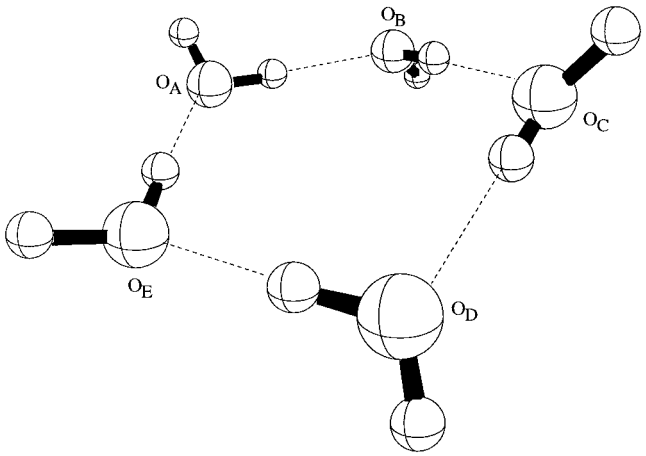

Figure 1. The asymmetric equilibrium structure of the cyclic water pentamer. The R_{O-O} distances are 2.729, 2.726, 2.726, 2.724, and 2.731 Å from O_A to O_E.[17] The respective hydrogen bond angles (∠O−H···O) are 176.2°, 176.0°, 175.8°, 173.3°, and 177.1°. The out-of-plane flipping angles of the free hydrogens attached to the oxygens from O_A to O_E can be expressed as the dihedral angle between individual monomer plane and the plane formed by the monomer oxygen and its two adjacent oxygens, since the oxygen ring is puckered; these are 53.0°, 55.3°, 52.2°, 58.9°, and 36.4°, respectively, as measured from the geometry calculated by Xantheas and Dunning.[15] The degree of puckering can be seen from the dihedral angles between the oxygen planes, which are 20.4° between the $O_A-O_B-O_D$ and $O_B-O_C-O_D$ planes and 2.1° between $O_A-O_B-O_D$ and $O_A-O_E-O_D$.[15]

spectrum results because "the tunneling splittings due to the flip exceed the range scanned experimentally to date".[61] Moreover, they put forth a detailed, molecular symmetry (MS) group theoretical description of the flipping and bifurcation rearrangements.

A manifold of pseudorotational states must occur as a result of the facile flipping rearrangement, as we learned in the case of the trimer, but this has not been treated in the above theoretical work. In the present paper, we propose a 5-D pseudorotation model analogous to the 3-D model recently developed for the cyclic trimer[40,41] to help assign the observed pentamer band and to predict new ones. Discussions regarding the lack of bifurcation tunneling splittings in $(D_2O)_5$ and the possibility of resolving them in $(H_2O)_5$ are also presented. Indeed, such splittings in $(H_2O)_5$ have actually been observed in recent experiments by Brown and co-workers.[62]

In this work, we employ a somewhat different (from W&W's, vide infra) group theoretical description with focus on the torsional dynamics to rationalize that the observed band is a pseudorotational transition. Such an assignment relies on the following experimental evidence: (1) the transition type, compared with the selection rules derived for both pseudorotation and overall rotation; the latter pertains directly to our spectral analysis, yet has not been pursued in the previous theoretical work; (2) the band origin; (3) the change in the rotational constants effected by vibrational excitation; and (4) most importantly, the averaged *symmetric* rotor behavior in both the ground and vibrationally excited states, despite the *asymmetric* equilibrium structure, which is believed to be the unequivocal spectroscopic proof of the involvement of pseudorotation.

II. Experimental Section

The Berkeley tunable terahertz laser spectrometer has been described previously.[63] Only the details pertinent to this study are given here. The pentamer signals reported in this work were observed only with a pulsed, instead of a cw, slit nozzle (101.6 mm × 0.100 mm with a throat depth of 3.175 mm).[64] Using argon as a carrier gas at a pulse repetition rate of 35−60 Hz, we observed the optimal pentamer signal at a background pressure of 30 mTorr and a backing pressure of 1.5−2 atm. Helium and 70% Ne balanced with helium were also used as carrier gases to verify that the spectral carrier was not a rare-gas complex; the corresponding background pressures were 200−800 and 120−220 mTorr, respectively. As shown in Figure 2, the Doppler limited line widths associated with helium and the Ne/He mix are broader than those observed with argon. The narrow line width and low operating background pressure are the two main advantages that argon offers as the carrier gas.

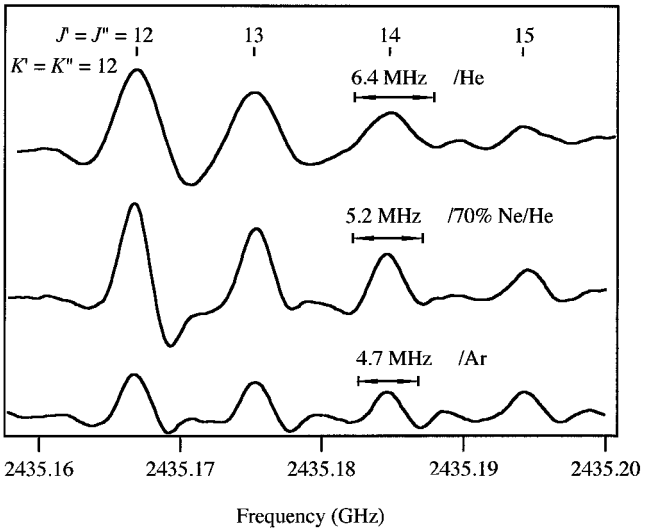

Figure 2. Experimental VRT spectra of the $K = 12$ subband of Q branch transitions of $(D_2O)_5$ obtained with three different carrier gases: Ar, 70% Ne mix with He, and pure He.

Attempts to measure the pentamer dipole moment through the Stark effect, as recently accomplished for the water hexamer,[65] have not been successful. An electrical field up to 45 V cm^{-1} was applied between the nozzle body (grounded) and a wire electrode placed in front of and parallel to the slit. This configuration has produced measurable shifts (5 MHz) and splittings on certain $(H_2O)_2$ transitions,[66] but not on those of $(D_2O)_5$ observed in this work as explained below.

Improvements on the previous strategy[3] to identify the size (n) of the cluster using the isotope mixture have been made as follows. For the pure, rather than isotopically mixed,[7] D_2O clusters, the line intensity (I) is related to the D mole fraction (f_D) through

$$I \propto (f_D)^{2n} \tag{1}$$

To avoid the long-term drift in the signal, we chose the normalized intensity I/I_0 and mole fraction $f_D/f_{D,0}$ by alternately measuring the signals of the sample (I) and a reference solution (I_0) of known mole fraction ($f_{D,0} = 99.9\%$, Cambridge Isotopes). As shown in Figure 3, a nearly zero intercept in the logarithmic plot of eq 1 suggests that the kinetic isotope effects are negligible within the range of mole fraction variation ($\Delta f_D \sim 16\%$) employed in this work. Such a plot for the $(D_2O)_5$ absorption yielded a cluster size n of 5.14 ± 0.36 at the 95% confidence level. The validity of this mixture test has also been established for VRT spectra of the water dimer, pure and isotopically substituted trimers,[7] tetramer,[8] and hexamer.[10]

The pentamer transitions appear as featureless singlets, so the use of the isotope mixture test was critical to discriminate the pentamer signals from the absorptions from many other

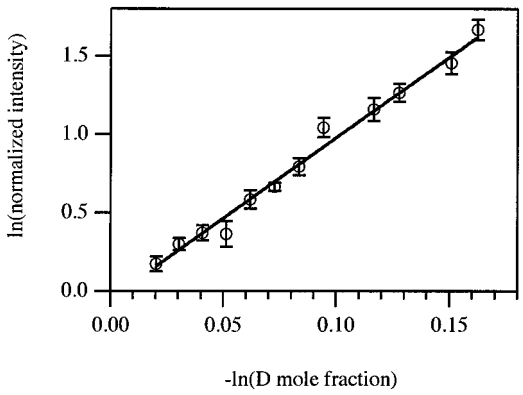

Figure 3. The result of the isotope test used to establish the cluster size ($n = 5.14 \pm 0.36$) of the spectral carrier. Each data point represents at least 10 normalized intensity measurements. The slope should be twice the cluster size. The nearly zero intercept (-0.049 ± 0.030) is a test of the validity of this model and evidence that perturbations such as kinetic isotope effects are negligible.

clusters coexisting in the jet. Due to the spectral congestion encountered in this frequency range, as shown in Figure 4, literally all the $(D_2O)_5$ transitions reported here have been tested. The isotope test, however, only establishes the cluster size. The detailed structure determination comes from the analysis of the rotational constants presented below.

III. Spectral Assignment

Figure 5 shows the actual spectrum of the $(D_2O)_5$ *Q* branch progressions resembling the parallel ($\Delta K = 0$) transitions of a symmetric top. Because only the difference in the rotational constant *A* (for a prolate) or *C* (for an oblate) between the ground and excited states can be uniquely determined in a parallel band, the type of symmetric rotor was determined by simulating the carefully measured intensity profiles of the *Q* branch region (Figure 6). By varying the ratio of this unique rotational constant to the average *B* value between the prolate and oblate limits, while maintaining the same difference ΔA or ΔC, we found that when both the Boltzmann ($T_{rot} = 5$ K) and Hönl−London factors were considered, the observed intensity profiles (Figure 6) can only be well reproduced by using $2C \sim B$ ($=A$), indicating a nearly planar oblate rotor. Such a method was also adopted in the analysis of the parallel band of $(D_2O)_4$.[8]

Based on the above approach, a total of 217 VRT transitions (available in archival form) were fit to the Hamiltonian for an oblate symmetric rotor. The resulting molecular parameters are listed in Table 1.

IV. Structural Characterization

A number of different structures have been identified in theoretical studies of the water pentamer. There is consensus among the ab initio calculations that the global minimum is an asymmetric (C_1) quasiplanar homodromic ring.[15,17,25,59,61] Previous studies of the pentamer structures and energetics made with the use of empirical potential surfaces, however, tend to produce conflicting results regarding the stability of the cyclic form.[56−58,60,67,68] Recent MD simulations of the intermolecular vibrational spectra of water clusters in the 0−1000 cm^{-1} frequency range by Bosma, Fried, and Mukamel using the enhanced simple point charge (SPC/E) model potential[69] found that the ring configuration of pentamer was preferred even as the temperature was raised—only more puckering of the ring occurred.[31] It is remarkable that these authors observed the room-temperature oxygen−oxygen radial distribution function of the pentamer to possess a second peak (which is often a criterion for judging the quality of the effective pair potential employed in liquid water simulations) around 4.25 Å, close to that found for liquid water at 310 K.

Our structural analysis proceeds from the precisely measured vibrationally averaged rotational constants that are characteristic of a nearly planar oblate rotor ($A = B \sim 2C$). Considering the above theoretical structures, we find that only the ring form satisfies this basic inertial mass distribution. Moreover, the calculated equilibrium structure is *asymmetric* (point group C_1) due to the uneven alternation of the free hydrogens above and below the oxygen ring and slight puckering of the ring, whereas the observed spectrum is that of a perfect symmetric top (effective C_{5h} structure).

The dynamical symmetry of the cyclic pentamer could also be attributed to a minimum geometry corresponding to all the

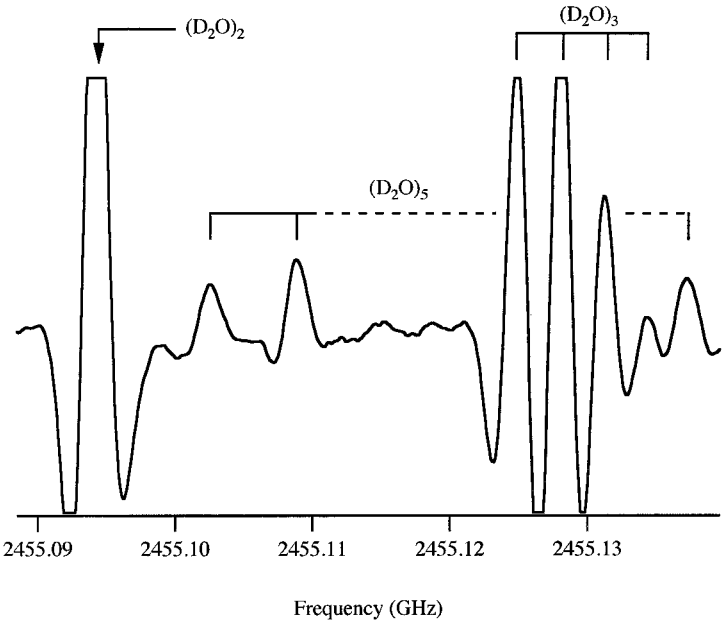

Figure 4. An example of the spectral congestion encountered in this work. A 50 MHz scan shows the absorption signals from the D_2O dimer, trimer, and pentamer. Partial and full overlap of strong dimer or trimer signals with the weak pentamer absorption has also been observed, which indicates the necessity of very high resolution in experiments not employing explicit mass selection.

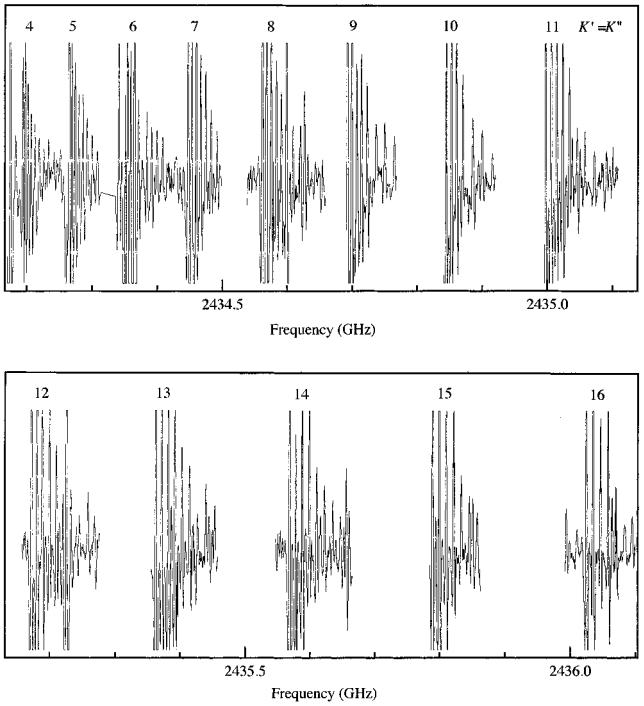

Figure 5. The experimental VRT spectrum of the $K = 4$ to 16 subbands of Q branch transitions.

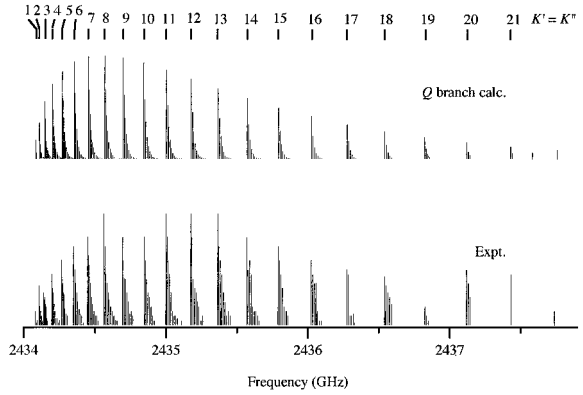

Figure 6. The experimental and calculated stick spectra of $(D_2O)_5$ in the Q branch region. Even at the planar oblate limit ($2C'' = B'' = A''$) the calculated profile still peaks at the subbands with $K = 7$, 8, and 9 that are lower than the experimental maxima (up to $K = 13$). This slight mismatch actually reinforces the structural assignment of $(D_2O)_5$ to a quasiplanar ring because a nonplanar condition ($2C'' > B'' = A''$) toward the spherical top or prolate limit would lead to a shift of intensity maxima toward even lower K stacks. Conversely, a better intensity agreement would require $2C'' < B'' = A''$, a relation which does not correspond to a physical object!

hydrogens lying either in, or on the same side ("crown") of, a plane formed by five oxygens. However, previous observations of the water trimer, wherein all three constants were obtained in a perpendicular band,[4] showed that the out-of-plane flipping motion is associated with a large negative inertial defect, thereby ruling out the stationary planar structure. A crown trimer lies at a higher energy (317.3 cm^{-1} above the global minimum according to the ab initio studies of Leutwyler and co-workers using the coupled-cluster method[20,21]) and thus not expected to be significantly populated in a supersonically cooled jet. In the case of the pentamer, although we do not have the absolute value of the C constant to quantify the degree of planarity, it is nevertheless unlikely that the structure is either rigorously planar or crownlike.

Even if the C constant were directly available from the spectroscopic analysis, it still should not be taken directly as a rigorous structural constraint if it is obtained in a standard semirigid symmetric top Hamiltonian analysis, such as that employed here. There are other dynamical effects, such as the Coriolis coupling between the overall rotation and the flipping motions responsible for the VRT transitions, to consider before one can interpret it structurally. Again taking the trimer as an example, we find that the C constant cannot be reproduced exactly without unreasonably distorting the structure in a Monte Carlo (MC) simulation which incorporates the flipping motions.[7] This is because the C constant is badly contaminated by the Coriolis effect associated with pseudorotation, for which the internal rotational quantum number (k) couples to the projection of the overall rotation along the c-axis (K_c), as described previously.[4] However, this effect was *not* explicitly treated in the rotational Hamiltonian employed to obtain the only experimentally available C constant from the perpendicular $(D_2O)_3$ band at 98.1 cm^{-1}.[4] Recently, van der Avoird and co-workers have formulated a detailed treatment of this Coriolis coupling mechanism[40] and have successfully interpreted the accompanying experimental spectral features.[41]

TABLE 1: Molecular Constants (in Megahertz) Obtained in a Fit of the $(D_2O)_5$ Transitions Reported in Archival Form[a]

Molecular Constants								
			ground state			excited state		
$A = B$			1750.815(76)			1751.163(76)		
$\Delta C = C' - C''$			7.6155(86)					
D_J			0.00159(48)			0.00163(48)		
D_{JK}			−0.0048(15)			−0.0048(15)		
ν_0 (band origin)			2 434 074.36(55)					
Correlation Matrix								
A''	1.00							
A'	0.99	1.00						
ΔC	−0.10	−0.12	1.00					
ν_0	0.22	0.13	−0.39	1.00				
D_J''	0.83	0.86	−0.22	0.15	1.00			
D_J'	0.82	0.85	−0.23	0.12	1.00	1.00		
D_{JK}''	0.07	0.03	0.21	0.10	−0.33	−0.34	1.00	
D_{JK}'	0.07	0.03	0.22	0.11	−0.34	−0.35	1.00	1.00

[a] Root-mean squares error of the fit is 3.4 MHz. the correlation matrix is also listed. The 2σ uncertainties in the last digits of the parameters are given in the parentheses.

Based on the above discussion, our structural characterization of the pentamer ring is derived from only two experimental constraints: the precisely measured A and B ($=A$) constants, which are primarily determined by the positions of the heavy oxygen atoms; the detailed hydrogen coordinates cannot be determined using the method described below, not only because of the limited experimental constraints but also more fundamentally due to the facile large amplitude flipping motions of the free protons. Therefore, we approximated the vibrationally averaged structure by a planar equilateral pentagon with a point mass of 20 amu (m_{D_2O}) at each apex so that the center-of-mass separation (R_{com}) can be uniquely solved to satisfy the expression

$$I_A = I_B = {}^5/_8 m_{D_2O} R_{com}^2 \csc^2(\pi/5) \qquad (2)$$

where I_A and I_B are the moments of inertia. To obtain the averaged inter-oxygen distances, R_{O-O}, we scaled R_{com} for the pentamer by 0.977, an empirical number determined from modeling the water dimer with the same point-mass method and subsequently scaling the dimer R_{com} to reproduce its experimental O−O distance of 2.98 Å.[45] The scaled pentamer R_{O-O} is 2.76 Å. The experimental R_{O-O} of the cyclic $(H_2O)_3$, $HOD(D_2O)_2$ with the H being free, $(D_2O)_4$ and a cage $(H_2O)_6$ [10] have also been obtained in similar fashion. It was later found in a MC simulation[7] of the trimer structure which considered

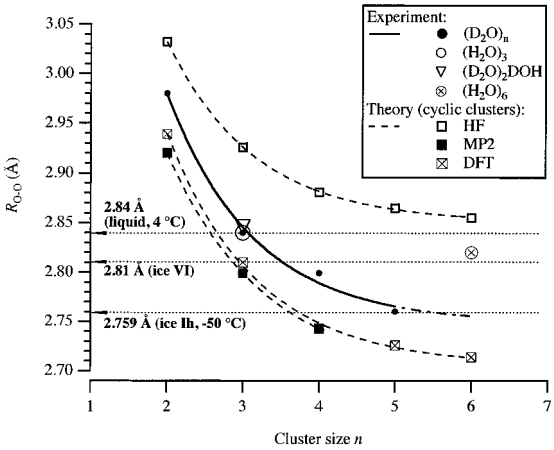

Figure 7. Comparison of the experimental and theoretical[15,17] interoxygen distance R_{O-O} as a function of the cluster size. The experimental trimer values and accordingly the fitting curve were improved from our previous work.[9]

the flipping motion that R_{O-O} of $(D_2O)_3$ was still overestimated by 0.045 Å in the point-mass model. Moreover, the MC simulation of the trimer showed that R_{O-O} varied by only 0.003 Å between $(D_2O)_3$ (2.837 Å) and $(H_2O)_3$ (2.840 Å). It is therefore expected that the structural parameters of $(H_2O)_4$ and $(H_2O)_5$ would not be much different from the values for their perdeuterated forms. We used these new trimer values in the R_{O-O} plot below (Figure 7).

We stress that the experimental R_{O-O} derived here from the measured rotational constants represents the vibrationally averaged O−O separation at the zero-point level, which should be longer than the values corresponding to the geometries at the potential minima. Consequently, the agreement between the experimental R_{O-O} with the MP2 and DFT equilibrium $R_{O-O}^{(e)}$ predictions by Xantheas and Dunning[15] and Xantheas[17] is much better than it appears to be in Figure 7. Recent DQMC calculations performed by Sorenson, Gregory, and Clary[70] to rigorously simulate the zero-point averaging effect yielded R_{O-O} of 2.84 and 2.85 Å for $(D_2O)_3$ and $(H_2O)_3$, respectively, in concert with our MC results.[7] These employed the empirical ASP-3B W2 (including multipoles up to rank 2) potential, which is a three-body (induction and Axilrod−Teller dispersion) modification of the original Millot and Stone anisotropic site potential (ASP)[71] developed from ab initio monomer properties using intermolecular perturbation theory. Although these researchers considered this close agreement fortuitous, the qualitative increase of the averaged O−O distance from the equilibrium value has been clearly demonstrated. Using a similar method, Gregory and Clary (G&C)[72] have obtained the vibrationally averaged center-of-mass separation (2.802 ± 0.005 Å) for $(D_2O)_5$. Fitting the experimental $R_{O-O}^{(n)}$ as a function of the cluster size *n* resulted in the following exponential relation

$$R_{O-O}^{(n)} = 2.748 + 1.3 \exp(-0.8644n) \qquad (3)$$

The similar R_{O-O} contraction toward the bulk values apparent in both experiment and theory quantifies the well-known "cooperative" effects in the hydrogen-bonding network and provides a means for untangling the important many-body interactions in bulk water potentials that are the source of this contraction.[72]

It is noteworthy that extrapolation of eq 3 to the cyclic hexamer yields a R_{O-O} of 2.756 Å, a value close to that of the hexagonal phase (Ih) of ice. This, in conjunction with their structural similarity (hexagonal H-bonding arrangement), adds further impetus for the study of the cyclic hexamer. On the other hand, our recent work on the cage hexamer[10] (see accompanying paper[65]) showed that its O−O distance deviated from the exponential trend established by the translinear dimer and cyclic clusters. The average value of 2.82 Å for the cage resembles the R_{O-O} of 2.81 Å for the high-density ice VI as determined using X-ray diffraction.[73] Moreover, the hydrogen-bonding network established in the noncyclic cage hexamer is also the same as that of the basic unit of ice VI.[74]

V. Dynamic Symmetry G_{10} and Pseudorotation

We now discuss the details of the quantum tunneling dynamics in the water pentamer-d_{10}, which are reflected in both the observed symmetric top structure and the absence of tunneling splittings in the spectrum. W&W first investigated two low-energy rearrangement mechanisms—flipping and bifurcation tunneling—in the pentamer.[61] However, flipping in that work, or pseudorotation preferred in this paper for the reasons discussed below, was not considered as the origin of the observed transition.

Our spectroscopic evidence—averaged symmetric rotor behavior in both the upper and lower states, combined with the ab initio consensus on the asymmetric equilibrium structure for the pentamer—suggests that pseudorotation through out-of-plane flipping (free OH bonds) and puckering (oxygen ring) motions must be responsible for the observed rovibrational transitions, based on the selection rules presented below (also see section VII, Discussion). This would lead to a manifold of states somewhat similar to those encountered in the case of a hindered rotation,[75] which cannot be fully characterized by the perturbative tunneling model of W&W.[61] The latter is more appropriate for high barrier tunneling motions such as bifurcation. For the flipping and puckering motions, although the MS groups employed to classify the state symmetries are the same or isomorphic in the two pictures, there are qualitative differences regarding the energy calculations and detailed transition selection rules. (1) The tunneling model of W&W can only predict the number of levels equal to the order of the MS group, e.g., 10 for the pentamer (C_{5h} or G_{10}) with certainty degeneracies; this restricts their model from predicting transition frequencies beyond the maximum tunneling splitting ($4|\beta_f|$ using their notation). (2) The rotational selection rules that one could derive by following the group theoretical treatment of W&W[61] would be insufficient to distinguish detailed $\Delta K = +1$ and $\Delta K = -1$ transitions, but the MS group described below does, which would become important in assigning perpendicular transitions involving Coriolis perturbations, as found in the water trimer.[3,5]

For the reasons discussed above, we choose a slightly different group theoretical description to better incorporate the pseudorotation model for the flipping−puckering dynamics. Since similar approach has been given in the recent trimer work by van der Avoird and co-workers,[40] we only summarize the results for the pentamer. The main difference here is that the MS group is G_{10} (isomorphic to C_{5h}), instead of G_6 for the trimer.

V.I. The MS Group G_{10}. First, we introduce our notation. The symbol u or d has the similar meaning to that described in the trimer[19,40] to designate the state of free D atoms being above or below a O···O···O plane, respectively, with the understanding that this plane is rigorously defined by the designated oxygen and its two nearest neighboring oxygens, since the pentagonal ring is puckered.

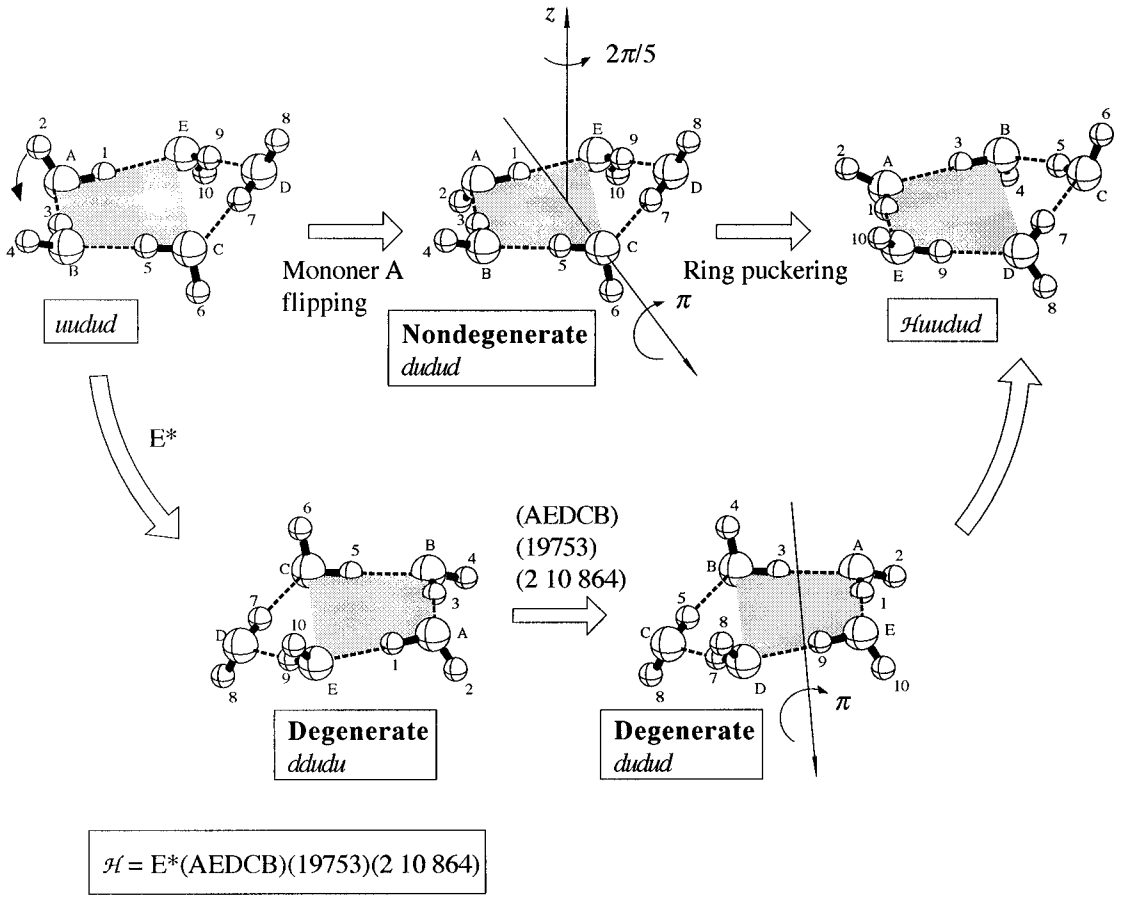

Figure 8. The schematic diagram of the single proton flipping pathway in the cyclic pentamer. The top route illustrates the pathway itself, while the bottom shows the equivalent effect of H. The curved arrow on monomer A of the starting geometry, *uudud*, indicates the direction of flipping. The shaded area represents the plane approximately formed by four oxygens. Note that the dihedral angle between the two oxygen planes $O_C\cdots O_D\cdots O_E$ and $O_B\cdots O_C\cdots O_E$ (O_A is approximately in this plane) is about 20°. Unlike in the trimer, to reach a degenerate version of the initial structure *uudud*, the puckered oxygen ring requires an extraframework motion for the starting ABCE plane in *uudud* to be the chiral image of the AEDB plane in *Huudud*, which could be concerted with the proton flipping. The single-proton flipping alone, as shown in the second structure along the top route, only produces a structure that is nondegenerate to *uudud*.

TABLE 2: The Effect of H^n on the Structure *uudud*[a]

n	structure	n	structure	n	structure	n	structure
0	*uudud*	3	*duddu*	6	*ududu*	8	*uduud*
1	*dudud*	4	*duudu*	7	*ududd*	9	*uddud*
2	*duduu*	5	*ddudu*				

[a] Note that the structures corresponding to $|n_1 - n_2| = 5$ are inverted relative to each other because $H^5 = E^*$.

TABLE 3: Definition of the Irreps of G_{10} ($\equiv C_{5h}$) and the Corresponding Characters under the Operation H^n [a]

irreps	A_1^+	A_1^-	A_2^+	A_2^-	A_3^+	A_3^-	A_4^+	A_4^-	A_5^+	A_5^-
k (mod 10)	0	5	−4	1	2	−3	−2	3	4	−1
Character $\chi^{(k)}(H^n)$	$\exp((nk\pi/5)i)$									

[a] The pseudorotational state symmetry is labeled by its quantum number k.

Next, we briefly describe the MS group G_{10}. It is generated by the cyclic operations of $H \equiv$ (AEDCB)(19753)(2 10 864)* $\equiv E^*$(AEDCB)(19753)(2 10 864), where E^* is the spatial inversion operation. The effect of H on one labeled equilibrium structure, *uudud* (in the monomer ordering of ABCDE that is held fixed throughout), has been diagrammed in Figure 8. Defining H^n as H operating n times, we have summarized in Table 2 the effect of H^n on an initial structure, *uudud*. The irreducible representations (irreps) of G_{10} and their corresponding characters $\chi^{(k)}(H^n)$ under the operation H^n are listed in Table 3, where k is the internal rotation or pseudorotation quantum number. As shown in Figure 9, each application of H rotates the principal inertial system about the approximate c-axis by $-2\pi/5$. Hence the term "pseudorotation" appertains, as this process is symmetrically equivalent to the overall rotation about the c-axis. It can be shown[40] that using Table 3 the complete pseudorotation−overall rotation selection rule is simply $(-k' + K' + k - K) = 10n + 5$, where n is an integer, since the transition dipole operator, the pseudorotation wave function Φ_k, and the overall rotation wave function $|JKM\rangle$ (normalized Wigner D^* function) transform in G_{10} as A_1^- [character (mod 10) = 5], labels k and $-K$, respectively.

It is noteworthy that the detailed rotational selection rules are different between $\Delta k = -4$ (A_2^+) ← 0 (A_1^+) and 4 (A_5^+) ← 0 (A_1^+), even though the $k = \pm 4$ levels are accidentally degenerate (but irreducibly degenerate in W&W's treatment) in the model presented below; the former corresponds to $\Delta K = K' - K = +1$, the latter $\Delta K = -1$. Both are regarded as being of perpendicular type, but they are clearly different rotational transitions in practical spectroscopic assignments. This becomes especially important when these accidentally degenerate levels are split by Coriolis coupling between the internal and external rotations, which has been observed in the trimer,[3,5] yet has not been clearly elaborated in the past. In that case, the selection rules need to be adapted to the MS group G_6 ($\equiv C_{3h}$) so that $(-k' + K' + k - K) = 6n + 3$. Due to this difference in rotational selection rules within the accidentally degenerate states, which would otherwise be obscured using the customary $E_{1,2}'$, $E_{1,2}''$ labels proposed by W&W,[61] we see the necessity

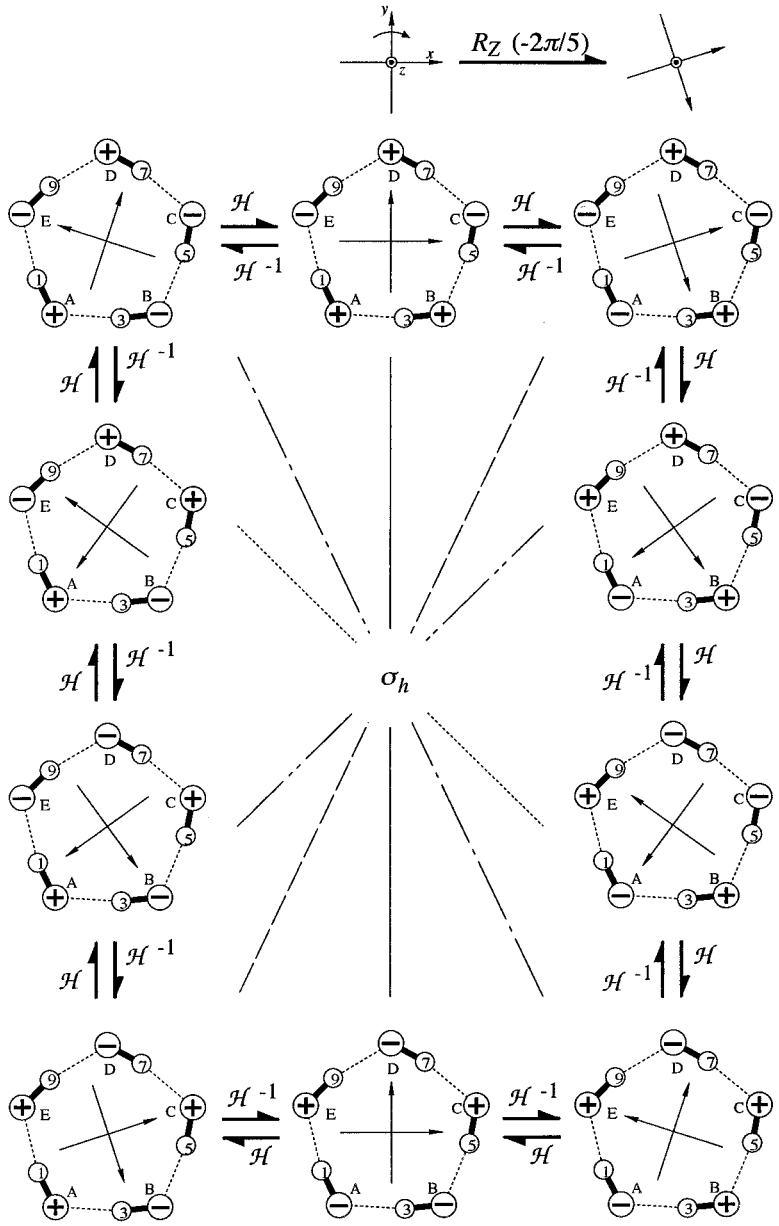

Figure 9. A schematic diagram to illustrate the pseudorotation model. The 10 degenerate structures are successively linked by the single proton flipping pathway corresponding to the generator H and its inverse operation H^{-1}. Each operation of H rotates clockwise the principal inertial axis system, superimposed on each structure and shown at the top of the diagram, by $-2\pi/5$ about the z axis pointing above the plane (σ_h). The signs on the oxygen atoms denote their positions and also the states of the free hydrogens attached to these oxygens being above(+) or below(−) the plane. These signs change along the path also due to the ring puckering motion. The concerted multiple proton flipping pathways would link structures within these 10 versions, e.g., the concerted five-proton flipping pathway connects the two structures linked by the lines of the same kind through the center label σ_h, which is equivalent to E^* ($=H^5$).

for distinguishing them using the group G_{10} described in this work (Figure 10).

V.II. The Pseudorotation Model. Last, the torsional energy levels of the pentamer can be predicted using a 5-D pseudorotational Hamiltonian similar to that formulated for the trimer.[40] The degrees of freedom are related to the five internal rotational angles of the flipping monomers $\chi = \{\chi_\alpha | \alpha = A, B, C, D, E; -\pi < \chi_\alpha \leq \pi\}$; $\chi_\alpha = 0$ corresponds to the free proton located in the plane formed by O_α and its two nearest neighbor oxygens. Neglecting the coupling between pseudorotation and overall cluster rotation, we can write the Hamiltonian as

$$H_{\text{int}} = -F \sum_\alpha \frac{\partial^2}{\partial \chi_\alpha^2} + V(\chi_A,\chi_B,\chi_C,\chi_D,\chi_E) \qquad (4)$$

where F is the reduced internal rotational constant and $V(\chi_A,\chi_B,\chi_C,\chi_D,\chi_E)$ is the 5-D torsional potential energy surface. For the trimers, different values of F have been obtained upon different choices of the torsional axis.[19,38,39,41] Neglecting the effect of puckering on F, our calculation, based on the donor O−H bond as the torsional axis, produced F of 10.09 cm^{-1} for $(D_2O)_5$ and 20.11 cm^{-1} for $(H_2O)_5$, which are only slightly

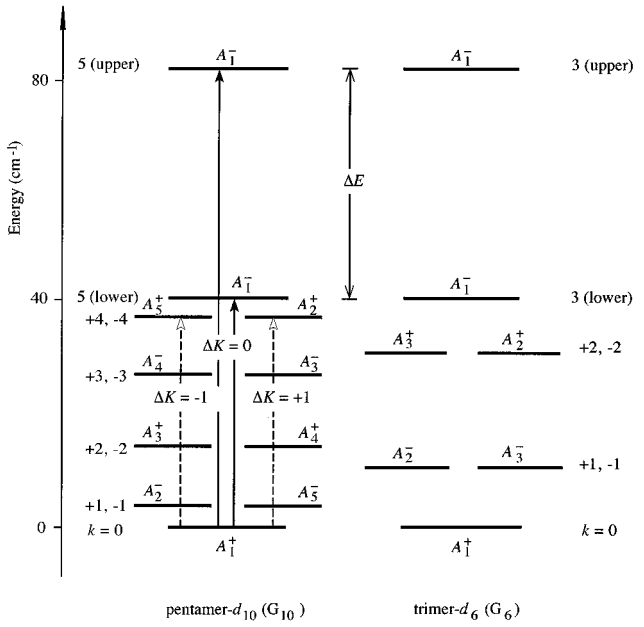

Figure 10. Schematic comparison between the pseudorotational energy levels in $(D_2O)_3$ and those crudely proposed for $(D_2O)_5$. The $k = n$ (upper) ← n (lower) (n = cluster size) splitting is denoted by ΔE. Two types of strongly allowed pseudorotational transitions, $\Delta k = 5 \leftarrow 0$ and $\pm 4 \leftarrow 0$, are shown with the reliable, accompanying overall rotation selection rules. Note that $\Delta k = +4$ and $-4 \leftarrow 0$ are associated with different rotational selection rules, $\Delta K = -1$ and $+1$, respectively, although both are considered to be of perpendicular type; this becomes important when the accidental degeneracy of the $k = \pm 4$ levels is removed by Coriolis mixing between the pseudorotation and overall rotation.

different from the corresponding trimer values, 10.23 and 20.27 cm^{-1} for $(D_2O)_3$ and $(H_2O)_3$, respectively.

It can be shown that for the lowest 10 pseudorotational states with $k = 0, \pm 1, ..., \pm 4, 5$, the energy expression is

$$E_k = \frac{E^{(0)} + 2\beta \cos(k\pi/5)}{1 + 2S \cos(k\pi/5)} \tag{5}$$

where

$$E^{(0)} \equiv \langle uudud|H_{\text{int}}|uudud\rangle$$

$$\beta \equiv \langle uudud|H_{\text{int}}|dudud\rangle = \langle uudud|H_{\text{int}}|uddud\rangle$$

$$S \equiv \langle uudud|dudud\rangle = \langle uudud|uddud\rangle = \langle u|d\rangle \tag{6}$$

and $|uudud\rangle$ is the localized basis function corresponding to the potential minimum *uudud*. The associated symmetry adapted function $|\Phi_k\rangle$ for a given k is

$$|\Phi_k\rangle = \frac{1}{\sqrt{10}} \sum_{n=-4}^{5} \exp\left(-\frac{nk\pi}{5} i\right) H^n |uudud\rangle, \quad k = -4, ..., 5 \tag{7}$$

Note in eq 5 that the lowest six energy levels (two nondegenerate and four doubly degenerate) agree with the result of W&W's perturbation model when the overlap integral S is neglected. However, the perturbation model[61] cannot predict higher energy levels, whereas the pseudorotation model can simply by employing a larger basis $|\Phi_k\rangle$ and then solving eq 4.

We stress that the simple pseudorotational model here is only intended to provide an order-of-magnitude estimate on the energetics, due to the current lack of a 5-D torsional surface required to perform the numerical calculations. On the basis of our knowledge of the trimer system, the energy pattern in the pentamer can be crudely quantified as follows.

To calculate the lowest six pseudorotational levels ($k = 0, \pm 1, ..., \pm 4, 5$) according to eq 5, we need to evaluate the parameter β. W&W[61] have reported the β values for $(H_2O)_5$ and $(D_2O)_5$ to be -4.5 and -3.2 cm^{-1}, respectively, which they found not significantly different from the corresponding elements in the trimer. Empirically, β for $(H_2O)_3$ and $(D_2O)_3$ can be estimated to be one-fourth of the negative transition frequencies -41.1 and -87.1 cm^{-1}, respectively.[38,39,41] We argue that the trimer β values are somewhat comparable to those of the pentamer, based on the theoretical results[61] and the following two counterbalancing effects. (1) The requirement of heavy oxygen ring puckering motions in the degenerate flipping pathway would lead to a similar F in eq(4) and consequently smaller $|\beta|$ than that for the trimer. (2) Less strain in the pentamer ring, due to the nearly tetrahedral O···O···O angle, and more vibrational degrees of freedom—larger zero-point energy—may effectively reduce the barrier to flipping and therefore yield larger $|\beta|$ for the pentamer. This subset of the pentamer pseudorotational energy levels (Figure 10) was thus constructed using the empirical $|\beta|$ value established for the trimer, although the above assumption clearly should be examined in future theoretical work.

For the higher pseudorotational states, e.g., $k = 5$ (upper) [the upper k value shown here is essentially k (mod 10) with $k = -5$] in Figure 10, we also resorted to the trimer system for an order-of-magnitude estimate. In a simplified 1-D pseudorotation model, wherein the potential is approximated as $V_{2n}/2[1 - \cos(2n\chi)]$,[6,19,75] the splitting between $k = n$ (lower) and n (upper) levels (n = cluster size) is identical for the trimer and pentamer at the same barrier height V_{2n}. We therefore assume the $k = 5$ (upper) ← 5 (lower) spacing in the pentamer to be at least comparable to the $k = 3$ (upper) ← 3 (lower) splitting in the trimer. The latter has been calculated by Olthof et al.[41] to be slightly larger than the $k = 3$ (upper) ← 0 spacing. This assumption was adjusted according to the assignment made below.

Figure 10 summarizes the pseudorotational energy levels of $(D_2O)_5$ in comparison with those of $(D_2O)_3$. The $k = n$ (upper) ← n (lower) spacings are only roughly drawn to scale.

VI. Pseudorotational Assignment

We now attempt to assign the observed band according to (a) the approximate energetics but (b) relatively rigorous selection rules established in the above pseudorotation model. The 81.2 cm^{-1} $(D_2O)_5$ band measured in this work is likely to originate from the ground state with $k = 0$ since the absorption signal did not behave like a hot band in response to heating of the sample reservoir.

The highest frequency parallel band among the lowest $k = 0, \pm 1, ..., \pm 4, 5$ (lower) manifold is $k = 5$ (lower) ← 0. It is predicted to be only within 36.1−46.1 cm^{-1} for $(D_2O)_5$ on the basis of our approximation; the 10 cm^{-1} uncertainty (also placed on other transitions listed in Table 4) is given roughly according to the accuracy found in the pseudorotation model of the trimer. The $k = 5$ (lower) ← 0 assignment is therefore unlikely.

The next allowed parallel band which originates from the $k = 0$ ground state corresponds to $k = 5$ (upper) ← 0, which is expected to be comparable to the $k = 3$ (upper) ← 0 transition in the trimer. The latter was calculated to be 96.1 or 88.93 cm^{-1} depending on the choice of torsional potentials.[41]

TABLE 4: Low-Frequency Pseudorotational Transitions (in cm^{-1}) Predicted for $(H_2O)_5$ and $(D_2O)_5$[a]

k'	←	k	type	$(H_2O)_5$	$(D_2O)_5$
5 (lower)		0	//	82.1−92.1[b]	36.1−46.1[b]
5 (upper)		0	//	167.1−177.1	76.2−86.2[c] 81.2 (expt)
±4		0	⊥	73.8−83.8	32.2−42.2
			Hot Bands		
5 (lower)		±1	⊥	73.8−83.8	32.2−42.2
5 (upper)		±1	⊥	158.8−168.8	72.3−82.3
±4		±1	//	65.5−75.5	28.3−38.3

[a] The $k = 5$ (upper) ← 0 transition in $(H_2O)_5$ was estimated according to the ratio of the corresponding $(D_2O)_5$ band origin observed in this work to the predicted central frequency of the 5 (lower) ← 0 transition. The signs of // and ⊥ denote the parallel ($\Delta K = 0$) and perpendicular ($\Delta K = \pm 1$) rotational transition types, respectively. The respective $k = 1 \leftarrow 0$ separations in $(H_2O)_5$ and $(D_2O)_5$ are approximated to be 8.3 and 3.9 cm^{-1}. [b] The central frequencies are the band origins of the $k = 3 \leftarrow 0$ pseudorotational transition in $(H_2O)_3$ and $(D_2O)_3$. [c] Based on the observed band origin, 81.2 cm^{-1}, tentatively assigned in this work.

Other parallel transitions higher in frequency than the $k = 5$ (upper) ← 0 band would be $k = \pm 3$ (upper, A_4^-, A_3^-) or 5 (second upper, A_1^-) ← 0 (A_1^+). The first kind corresponds to $\Delta K = \pm 2$, which should not be strongly allowed. The second one would occur at a much too high frequency [~150 cm^{-1} on the basis of the $(D_2O)_3$ results[41]] to be a reasonable candidate.

Therefore, assigning the $(D_2O)_5$ band observed in this work to the $k = 5$ (upper) ← 0 pseudorotational transition appears to be most consistent with the model predictions. Table 4 summarizes the expected pseudorotational transitions associated with the proper overall rotational transition types for both $(D_2O)_5$ and $(H_2O)_5$. We considered only the transitions from the lowest pseudorotational levels (~10 cm^{-1} above the ground state, therefore the levels of $k = 0$ and ±1) which are likely to be significantly populated in the supersonically cooled molecular jet (thermal energy $kT \sim 7$ cm^{-1}). Since the transitions from $k = 0$ to $k = \pm 3, \pm 2, \pm 1$ would correspond to $\Delta K = \pm 2, \pm 3, \pm 4$, respectively, they are essentially forbidden. The transitions from nonzero accidentally degenerate k levels (hot bands) are expected to be perturbed by the Coriolis coupling between pseudorotation and the overall rotation [more severe for $(D_2O)_5$ due to its closer energy spacings than in $(H_2O)_5$], as we have learned from the recent extensive studies of the trimer.[40,41] Such perturbation was not obvious in our spectrum.

It is interesting that a recent search according to the predictions in Table 4 did lead to observation of a $(H_2O)_5$ perpendicular ($\Delta K = \pm 1$) or parallel (but $\Delta K = \pm 2$) band near 90 cm^{-1},[62] which is close to the predicted $k = \pm 4 \leftarrow 0$ or $k = 5$ (lower) ← ±1 transitions, although this could be coincidental without further detailed spectral analysis. The $\Delta K = \pm 2$ pseudorotational bands can be predicted, but these are not strongly allowed. Indeed, the intensity of the new band is weak.[62]

VII. Discussion

In their recent DQMC study of the cyclic water pentamer, Gregory and Clary[72] estimated the tunneling splittings associated with the single flipping and bifurcation mechanisms. A decrease in the splitting associated with flipping was found for the pentamer, compared with that for the trimer. The calculated values are 0.21 and 0.030 cm^{-1} for pentamer-h_{10} and -d_{10}, respectively.[72] Our own prediction of this splitting in $(H_2O)_5$ (8.3 cm^{-1}) and $(D_2O)_5$ (3.9 cm^{-1}) from the pseudorotation model could certainly be an overestimate. But judging from the DQMC results for the trimer-h_6 and -d_6, we anticipate an underestimate of this single flip splitting by the G&C treatment.

The β values evaluated for the pentamer were equally crude as the above splittings. But this does not invalidate the use of a pseudorotation model for our spectral assignment, nor is the accuracy of this single parameter crucial (only partially convenient) for describing all the complex experimental pseudorotational levels, as we have seen in case of the water trimer.[40,41] The spectral assignment proposed here could be incorrect due to the present lack of rigorous numerical calculations. However, the qualitative features and spectroscopic selection rules derived above from the pseudorotational model should be useful in future studies.

It is possible that the 81.2 cm^{-1} band is a combination band which must also involve pseudorotation. However, assigning the 81.2 cm^{-1} band to the pure pseudorotational transition, wherein the dominant motions are those of the light deuterons, is more consistent with (1) the observed small change ($\Delta \bar{B} = 0.35$ MHz) in the rotational constants upon vibrational excitation, and (2) the vibrationally averaged structure required by the C_{5h} symmetry to be a rigorous oblate top. Excitation of the stretching, e.g., the ring breathing mode, of the relatively stiff hydrogen bond would (a) introduce appreciable change in the distances between the heavy oxygen atoms, which would produce more than a few MHz change in the rotational constants according to our structural model, and (b) require higher energies. The H-bond stretching frequency is predicted to be 150 cm^{-1} for the dimer,[46] which should be even higher for the larger clusters as a result of increased stability per molecule through many-body interactions.[16,57] We point out that the ring puckering motion, though involving heavy oxygens, does not produce large change in $\bar{B}$ because $\bar{B}$ is less sensitive to the motions that are parallel to the inertial c-axis. There are other low-frequency nonstretching modes to consider, which intuitively would correspond to the oxygen ring motions, but these framework motions (twisting/bending) are themselves of pseudorotational character because the ring puckering motions participate in the pseudorotation pathway. The low-frequency translational modes alone[61] cannot produce the observation (2) listed above.

In addition, based on the complete pseudorotation-overall rotation selection rule, $\Delta K - \Delta k = 10n + 5$, we show that the likelihood of the VRT spectrum observed in this work being a special type ($\Delta k = 0$) of combination band, such as $|\nu', k' = 0\rangle \leftarrow |\nu, k = 0\rangle$, wherein $\upsilon' > \upsilon$ and both are the quantum numbers of certain vibration other than pseudorotation, is small. Since no other low-frequency intermolecular vibrational modes except for the 5-D pseudorotation are predicted to possess the C_{5h} symmetry, the symmetry of the vibrational (nonpseudorotational) wave function product in the transition dipole integral transforms as A_1^+. This would result in a weakly allowed rotational transition type of $\Delta K = \pm 5$, in contradiction to the observed $\Delta K = 0$ spectral signature. Therefore, with no change in k quantum number, the averaged symmetric top behavior observed in both the lower and upper vibrational states appears to necessarily require not only these states but also the transition between them to be of pseudorotational origin.

Our spectral assignment does not rely on the energetics alone. Because harmonic frequencies are predicted in the normal mode calculations on the basis of a single version of the equilibrium structure,[15] these cannot be directly compared with the experimental measurements on systems wherein pseudorotation dominates the dynamics. In the dimer and the trimer, the calculated harmonic frequencies are roughly a factor of 2 different from our experimental measurements considering only the energetics.

For the pentamer, there are a few normal modes of low frequencies that are close to the band origin of $(D_2O)_5$, e.g., those calculated by W&W (only given for the pentamer-h_{10}).[61] The eigenvectors (proportional to the vibrational amplitudes) associated with these low-frequency fundamental normal modes, however, cannot produce the averaged symmetric rotor behavior at the zero-point level, since the harmonic motions thus calculated do not interconvert different versions of equilibrium structures; in contrast, pseudorotation can explain such a behavior as well as other spectroscopic observations presented above. The possibility of observing a combination band of pseudorotation and other harmonic modes at the frequencies reported here has also been discussed above. In general, when the interconversion potential barrier along one particular normal coordinate is sufficiently low, such as the flipping and ring puckering in this highly nonrigid system, the corresponding harmonic frequency supported by a single potential well would inevitably evolve into a manifold of internal states, e.g., pseudorotation, as a result of interactions among degenerate minima on the multidimensional IPS, as in the simpler case of umbrella inversion in ammonia.

To interpret the experimental VRT spectra, one must solve for all the accessible states using either full dimensional intermolecular dynamical calculations, such as those performed for the small rare gas-free cluster systems such as $(HF)_2$,[76,77] $(HCl)_2$,[78,79] and $(NH_3)_2$,[80,81] or an adiabatic separation of the low-frequency torsions from other modes as carried out for the cases of the trimer[6,18,19,38−41,82] and pentamer.[61] The former is not computationally feasible. Despite the fact that the latter provides a semiquantitative understanding of the experimental observations,[4−7,18,19,38−41,61,82] expecting the pseudorotation model to produce frequencies in quantitative agreement with the experimental measurements is unrealistic, and beyond the validity of this adiabatic approximation. The fully coupled approach is ultimately required for this purpose.

The donor (bifurcation) tunneling splitting has thus far not been observed in the VRT spectrum of $(D_2O)_5$. This is consistent with the ab initio calculations of W&W,[61] even if theory had underestimated the splitting by 2 orders of magnitude. Compared with the already small ($\leq$5 MHz) bifurcation splittings measured for $(D_2O)_3$,[3−6] the absence of the corresponding splitting in $(D_2O)_5$ is not surprising if one considers two factors: (1) The involvement of heavy oxygen atoms in the bifurcation tunneling due to the puckering of the pentagonal ring, which is similarly required in the *degenerate* flipping pathway depicted in Figure 8, effectively increases the tunneling masses. (2) Since bifurcation tunneling requires the breaking of a H-bond, the enhanced stability per H-bond in the pentamer, resulting from many-body interactions, would inevitably play a key role in suppressing this motion.

The donor tunneling splittings could be observable in the $(H_2O)_5$ isotopomer, however. This was predicted by W&W to be 3 MHz,[61] which is discernible with our 1 MHz experimental resolution. Experimentally, the monotonic reduction of the splittings in progressing from $(H_2O)_2$ [83] to $(H_2O)_6$,[10] which appears to be well correlated with the enhanced H-bond strength with increasing cluster size (cooperativity), reasonably suggests that the bifurcation splitting in $(H_2O)_5$ would lie between the values of $(H_2O)_3$ (289 MHz,[4] a sum[40,41] of the splittings of the ground and excited states) and $(H_2O)_6$ (1.9 MHz,[10] a difference). If this is true, and neglecting the complications of the Coriolis effect, one would expect to see an equally spaced sextet (also predicted by W&W[61]) accompanying each rovibrational transition. Indeed, such splittings ($\sim$5 MHz adjacent line separation) were recently observed by M. G. Brown and co-workers in the $(H_2O)_5$ band.[62]

VIII. Conclusions

The parallel VRT band of $(D_2O)_5$ observed at 81.2 cm^{-1} has been analyzed in detail. The measured rotational constants are in best agreement with those predicted for a slightly puckered monocyclic ring form of the pentamer. The vibrationally averaged structure directly obtained in the experiment corresponds rigorously to a nearly planar oblate symmetric top, even though the predicted equilibrium structure is asymmetric due to the uneven alternate distribution of the free protons and the puckering of the oxygen ring. This behavior can be explained by the C_{5h} dynamical symmetry induced by the facile flipping motions (pseudorotation) of the monomers about their donor O−H bonds and by the accompanying hydrogen bond network puckering motions.

Calibrated structural modeling of the pentamer yielded a vibrationally averaged interoxygen distance R_{O-O} of 2.76 Å, which, together with the R_{O-O} calculated for the trans-linear dimer, cyclic trimer and tetramer, establishes an exponentially contracting trend that converges rapidly toward the corresponding value in normal ice (Ih) at a cluster size of 6. Excellent agreement exists between the experimental R_{O-O} trend and that predicted in the ab initio calculations of Xantheas;[15,17] the difference can be accounted for by zero-point effects.

A 5-D pseudorotation model is proposed in analogy to the 3-D model developed for the trimer to help assign the observed band of $(D_2O)_5$ and to predict new transitions. The empirical predictions serve as an order-of-magnitude estimate only for the absolute frequencies, but as a somewhat reliable guide for the relative transitions. On the basis of these and other spectroscopic evidence, we tentatively attribute the 81.2 cm^{-1} band to a $k = 5$ (upper) $\leftarrow$ 0 pseudorotational transition.

The donor tunneling motion responsible for the quartet splittings in the trimer is not feasible for $(D_2O)_5$, given the $\sim$1 MHz resolution limit of spectrometer. This is in concert with *ab initio* predictions.[61] On the basis of the monotonic decrease of this tunneling splitting found in progressing from the H_2O dimer, trimer, to hexamer, however, we may be able to observe it in $(H_2O)_5$, which is confirmed by our ongoing experiments.[62] Characterizing this splitting caused by breaking and making of the hydrogen bonds constitutes an important measure of the hydrogen bond cooperativity in the water pentamer.

Acknowledgment. This work is supported by the Experimental Physical Chemistry Program of the National Science Foundation (CHE-9424482). The authors would like to thank Prof. M. J. Elrod for helpful discussions.

Supporting Information Available: Assigned parallel transitions (in megahertz) of the vibrationally averaged oblate $(D_2O)_5$ cluster (5 pages). Ordering information is given on any current masthead page.

References and Notes

(1) Saykally, R. J.; Blake, G. A. *Science* **1993**, *259*, 1570.

(2) Pugliano, N.; Saykally, R. J. *J. Chem. Phys.* **1992**, *96*, 1832.

(3) Pugliano, N.; Saykally, R. J. *Science* **1992**, *257*, 1937.

(4) Liu, K.; Loeser, J. G.; Elrod, M. J.; Host, B. C.; Rzepiela, J. A.; Pugliano, N.; Saykally, R. J. *J. Am. Chem. Soc.* **1994**, *116*, 3507.

(5) Liu, K.; Elrod, M. J.; Loeser, J. G.; Cruzan, J. D.; Pugliano, N.; Brown, M. G.; Rzepiela, J.; Saykally, R. J. *Faraday Discuss. Chem. Soc.* **1994**, *97*, 35.

(6) Suzuki, S.; Blake, G. A. *Chem. Phys. Lett.* **1994**, *229*, 499.

(7) Liu, K.; Brown, M. G.; Viant, M. R.; Cruzan, J. D.; Saykally, R. J. *Mol. Phys.* **1996**, *89*, 1373 (special birthday issue honoring A. D. Buckingham).
(8) Cruzan, J. D.; Braly, L. B.; Liu, K.; Brown, M. G.; Loeser, J. G.; Saykally, R. J. *Science* **1996**, *271*, 59.
(9) Liu, K.; Brown, M. G.; Cruzan, J. D.; Saykally, R. J. *Science* **1996**, *271*, 62.
(10) Liu, K.; Brown, M. G.; Carter, C.; Saykally, R. J.; Gregory, J. K.; Clary, D. C. *Nature* **1996**, *381*, 501.
(11) Liu, K.; Cruzan, J. D.; Saykally, R. J. *Science* **1996**, *271*, 929.
(12) Mó, O.; Yáñez, M.; Elguero, J. *J. Chem. Phys.* **1992**, *97*, 6628.
(13) van Duijneveldt-van de Rijdt, J. G. C. M.; van Duijneveldt, F. B. *Chem. Phys.* **1993**, *175*, 271.
(14) Fowler, J. E.; Schaefer, H. F., III *J. Am. Chem. Soc.* **1995**, *117*, 446.
(15) Xantheas, S. S.; Dunning, T. H., Jr. *J. Chem. Phys.* **1993**, *99*, 8774.
(16) Xantheas, S. S. *J. Chem. Phys.* **1994**, *100*, 7523.
(17) Xantheas, S. S. *J. Chem. Phys.* **1995**, *102*, 4505.
(18) Wales, D. J. *J. Am. Chem. Soc.* **1993**, *115*, 11180.
(19) Schütz, M.; Bürgi, T.; Leutwyler, S.; Bürgi, H. B. *J. Chem. Phys.* **1993**, *99*, 5228.
(20) Bürgi, T.; Graf, S.; Leutwyler, S.; Klopper, W. *J. Chem. Phys.* **1995**, *103*, 1077.
(21) Klopper, W.; Schütz, M.; Lüthi, H.-P.; Leutwyler, S. *J. Chem. Phys.* **1995**, *103*, 1085.
(22) Kim, K.; Jordan, K. D.; Zwier, T. S. *J. Am. Chem. Soc.* **1994**, *116*, 11568.
(23) Tsai, C. J.; Jordan, K. D. *Chem. Phys. Lett.* **1993**, *213*, 181.
(24) Schütz, M.; Klopper, W.; Lüthi, H.-P.; Leutwyler, S. *J. Chem. Phys.* **1995**, *103*, 6114.
(25) Knochenmuss, R.; Leutwyler, S. *J. Chem. Phys.* **1992**, *96*, 5233.
(26) Mhin, B. J.; Kim, H. S.; Kim, H. S.; Yoon, C. W.; Kim, K. S. *Chem. Phys. Lett.* **1991**, *176*, 41.
(27) Mhin, B. J.; Kim, J.; Lee, S.; Lee, J. Y.; Kim, K. S. *J. Chem. Phys.* **1994**, *100*, 4484.
(28) Laasonen, K.; Parrinello, M.; Car, R.; Lee, C.; Vanderbilt, D. *Chem. Phys. Lett.* **1993**, *207*, 208.
(29) Chalasinski, G.; Szczesniak, M. M.; Cieplak, P.; Scheiner, S. *J. Chem. Phys.* **1991**, *94*, 2873.
(30) Pillardy, J.; Olszewski, K. A.; Piela, L. *J. Mol. Struct.* **1992**, *270*, 277.
(31) Bosma, W. B.; Fried, L. E.; Mukamel, S. *J. Chem. Phys.* **1993**, *98*, 4413.
(32) Cieplak, P.; Kollman, P.; Lybrand, T. *J. Chem. Phys.* **1990**, *92*, 6755.
(33) Franken, K. A.; Jalaie, M.; Dykstra, C. E. *Chem. Phys. Lett.* **1992**, *198*, 59.
(34) Vegiri, A.; Farrantos, S. C. *J. Chem. Phys.* **1993**, *98*, 4059.
(35) Gregory, J. K.; Clary, D. C. *J. Chem. Phys.* **1995**, *102*, 7817.
(36) Gregory, J. K.; Clary, D. C. *J. Chem. Phys.* **1996**, *103*, 8924.
(37) Gregory, J. K.; Clary, D. C. *Chem. Phys. Lett.* **1994**, *228*, 547.
(38) Klopper, W.; Schütz, M. *J. Chem. Phys.* **1995**, *237*, 536.
(39) Sabo, D.; Bacic, Z.; Bürgi, T.; Leutwyler, S. *J. Chem. Phys.* **1995**, *244*, 283.
(40) van der Avoird, A.; Olthof, E. H. T.; Wormer, P. E. S. *J. Chem. Phys.* **1996**, *105*, 8034.
(41) Olthof, E. H. T.; van der Avoird, A.; Wormer, P. E. S.; Liu, K.; Saykally, R. J. *J. Chem. Phys.* **1996**, *105*, 8051.
(42) Walsh, T. R.; Wales, D. J. *J. Chem. Soc., Faraday Trans.* **1996**, *92*, 2502.
(43) Ohmine, I. *J. Phys. Chem.* **1995**, *99*, 6767.
(44) Ohmine, I.; Tanaka, H. *Chem. Rev. (Washington, D.C.)* **1993**, *93*, 2545.
(45) Dyke, T. R.; Muenter, J. S. *J. Chem. Phys.* **1974**, *60*, 2929.
(46) Dyke, T. R.; Mack, K. M.; Muenter, J. S. *J. Chem. Phys.* **1977**, *66*, 498.
(47) Fraser, G. T. *Int. Rev. Phys. Chem.* **1991**, *10*, 189.
(48) Teeter, M. M. *Proc. Natl. Acad. Sci. U.S.A.* **1984**, *81*, 6014.
(49) Lipscomb, L. A.; Peek, M. E.; Zhou, F. X.; Bertrand, J. A.; VanDerveer, D.; Williams, L. D. *Biochemistry* **1994**, *33*, 3649.
(50) Niedle, S.; Berman, H.; Shieh, H. S. *Nature* **1980**, *288*, 129.
(51) van der Waals, J. H.; Platteeuw, P. C. *Adv. Chem. Phys.* **1959**, *2*, 1.
(52) Speedy, R. J. *J. Phys. Chem.* **1984**, *88*, 3364.
(53) Rahman, A.; Stillinger, F. H. *J. Am. Chem. Soc.* **1973**, *95*, 7943.
(54) Speedy, R. J.; Madura, J. D.; Jorgensen, W. L. *J. Phys. Chem.* **1987**, *91*, 909.
(55) Corongiu, G.; Clementi, E. *J. Chem. Phys.* **1993**, *98*, 2241.
(56) Vernon, M. F.; Krajnovich, D. J.; Kwok, H. S.; Lisy, J. M.; Shen, Y. R.; Lee, Y. T. *J. Chem. Phys.* **1982**, *77*, 47.
(57) Kim, K. S.; Dupuis, M.; Lie, G. C.; Clementi, E. *Chem. Phys. Lett.* **1986**, *131*, 451.
(58) Moore-Plummer, P. L.; Chen, T. S. *J. Chem. Phys.* **1987**, *86*, 7149.
(59) Burke, L. A.; Jensen, J. O.; Jensen, J. L.; Krishnan, P. N. *Chem. Phys. Lett.* **1993**, *206*, 293.
(60) Schröder, K. P. *Chem. Phys.* **1988**, *123*, 91.
(61) Wales, D. J.; Walsh, T. R. *J. Chem. Phys.* **1996**, *105*, 6957.
(62) Brown, M. G.; Keutsch, F.; Liu, K.; Saykally, R. J., unpublished results.
(63) Blake, G. A.; Laughlin, K. B.; Cohen, R. C.; Busarow, K. L.; Gwo, D.-H.; Schmuttenmaer, C. A.; Steyert, D. W.; Saykally, R. J. *Rev. Sci. Instrum.* **1991**, *62*, 1693.
(64) Liu, K.; Fellers, R. S.; Viant, M. R.; McLaughlin, R. P.; Brown, M. G.; Saykally, R. J. *J. Chem. Phys.* **1996**, *67*, 410.
(65) Liu, K.; Brown, M. G.; Saykally, R. J. *J. Phys. Chem. A* **1997**, *101*, 8995.
(66) Liu, K.; Brown, M. G.; Saykally, R. J., unpublished results.
(67) Owicki, J. C.; Shipman, L. L.; Scheraga, H. A. *J. Phys. Chem.* **1975**, *79*, 1794.
(68) Farantos, S. C.; Kapetanakis, S.; Vegiri, A. *J. Chem. Phys.* **1993**, *97*, 12158.
(69) Berendsen, H. J. C.; Grigera, J. R.; Straatsma, T. P. *J. Chem. Phys.* **1987**, *91*, 6269.
(70) Sorenson, J. M.; Gregory, J. K.; Clary, D. C. *Chem. Phys. Lett.* **1996**, *263*, 680.
(71) Millot, C.; Stone, A. J. *Mol. Phys.* **1992**, *77*, 439.
(72) Gregory, J. K.; Clary, D. C. *J. Chem. Phys.* **1996**, *105*, 6626.
(73) Kamb, B. *Science* **1965**, *150*, 205.
(74) Eisenberg, D.; Kauzmann, W. *The Structure and Properties of Water*; Oxford University: New York, 1969.
(75) Lister, D. G.; MacDonald, J. N.; Owen, N. L. *Internal Rotation and Inversion: An Introduction to Large Amplitude Motions in Molecules*; Academic Press: London, 1978.
(76) Quack, M.; Suhm, M. A. *Mol. Phys.* **1990**, *69*, 791.
(77) Quack, M.; Suhm, M. A. *J. Chem. Phys.* **1991**, *95*, 28.
(78) Elrod, M. J.; Saykally, R. J. *J. Chem. Phys.* **1995**, *103*, 921.
(79) Elrod, M. J.; Saykally, R. J. *J. Chem. Phys.* **1995**, *103*, 933.
(80) Olthof, E. H. T.; van der Avoird, A.; Wormer, P. E. S. *J. Chem. Phys.* **1994**, *101*, 8430.
(81) Olthof, E. H. T.; van der Avoird, A.; Wormer, P. E. S.; Loeser, J. G.; Saykally, R. J. *J. Chem. Phys.* **1994**, *101*, 8443.
(82) Sabo, D.; Bacic, Z.; Graf, S.; Leutwyler, S. *Chem. Phys. Lett.* **1996**, *261*, 318.
(83) Zwart, E.; ter Meulen, J. J.; Meerts, W. L.; Coudert, L. H. *J. Mol. Spectrosc.* **1991**, *147*, 27.